ROUGHNESS AND INERTIA EFFECTS FOR SLIDER AIR BEARINGS

Daniel Pantuso, Eduardo A. Repetto
IBM Argentina
Ing. Enrique Butty 275, 1300 Buenos Aires, Argentina

Luis G. Reyna
IBM Watson Research Center
P.O.Box 218, Yorktown Heights, New York 10598, U.S.A.

ABSTRACT:

We discuss the effects of disk roughness and inertia terms on the flying attitude of a air bearing slider of the type IBM 3380. The pressure acting on the bottom surface of the slider is determined by solving a modified Reynolds equation which includes a first order slip correction to take into account rarefied effects. The flying attitude is then determined from a balance of moments around the arm attachment point. It is found that the effect of disk roughness is rather small at the slider working conditions. The inertia effects increase the flying height for sliders at a skew angle of attack.

RESUMEN:

Discutimos los efectos de la rugosidad del disco y de los términos inerciales sobre la altura de vuelo en patines del tipo IBM 3380. La presión actuante sobre la cara inferior del patín se resuelve usando una modificación de la ecuación de lubricación de Reynolds, que incluye la corrección de primer order en la condición de no-deslizamiento debido al bajo número de Knudsen. La posición del patín se determina del balance de momentos alrededor del punto de pivote. Se encuentra que los efectos de la rugosidad son más importantes para velocidades bajas. Además, los términos inerciales aumentan la altura de vuelo y el ángulo de ataque.

1. INTRODUCTION

The hard disk magnetic recording technology relies on a self-acting air-bearing slider which keeps the read-write magnetic head at a very close distance to the recording surface. In the the 3380 type slider the air is compressed to about two atmospheres in its two taper areas to produce enough lift to keep the slider from scratching the recording surface. The taper angle is chosen so that the compression at the front of the slider is still present at very small disk velocities.

The flying attitude of the slider is obtained from the pressure acting on the air-bearing surface. This pressure is described by the Reynolds lubrication equation. The equation is an approximation to the compressible Navier-Stokes equations based on negligible vertical pressure gradients and temperature variations. A first order slip correction is introduced into the equations to take into account rarefied effects, see Burgdorfer [1]. At flying heights below 0.1μ the continuum approximation has to be discarded and a new equation is derived from the Boltzmann equations. The result of this analysis is a modified Reynolds equation (see Fukui et al. [2]).

The actual pitch angle, roll angle and flying heights are determined from a moment balance around the suspension point, see Deckert [3]. The pitch angle determines the reliability of the design, since it insures a compression area even if the pitch angle were to become negative. The minimum flying

height is one of the important parameters which determine the boundary width of the recorded bits. A smaller flying height usually leads to higher recording densities.

For a complete discussion of the tribology and mechanics of magnetic storage devices please refer to the recent book by Bhushan [4].

In this work solutions to the lubrication equations were obtained from a Finite Element Code which includes a simple mesh refinement strategy. The resulting equations were solved using a Newton's approach. The resulting system of non-linear equations, for the pressure and the angles were solved using a preconditioned GMRES method and sparse matrix techniques.

2. FORMULATION AND EQUATIONS

The Reynolds lubrication equation including the first order slip correction reads

$$\nabla\cdot[h^3p\nabla p + 6\lambda_m p_a h^2\nabla p - 6\mu V ph] = 12\mu\frac{\partial ph}{\partial t}. \tag{1}$$

Note that the divergence is taken only in the horizontal plane, see Fig. 1 for the coordinate system.

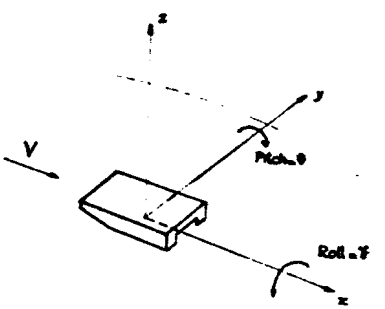

Fig. 1: Coordinate system

The term involving λ_m

$$\lambda_m = \lambda_a\frac{2-\sigma}{\sigma}.$$

arises from the slip correction to the Navier-Stokes equation. In the numerical results we use $\sigma = 0.9$ which corresponds to the slip coefficient of air on glass, see Bhushan pp.678 [4]. Slip coefficients for air on magnetic disk surfaces are not available. The Reynolds equation requires boundary data: it is customary to take Dirichlet boundary conditions and to impose the pressure to be the ambient pressure. See the work by Henshaw et al. for further discussion of this assumption [5].

The equations which determine the attitude of the slider are

$$m\frac{d^2h}{dt^2} + k_h\delta h = L_e + \int f dA \tag{2}$$

$$I_\theta\frac{d^2\theta}{dt^2} + k_\theta\delta\theta = P_e + \int(-fx + p\frac{\partial h}{\partial x}z_p)dA - S_x z_p \tag{3}$$

$$I_\gamma\frac{d^2\gamma}{dt^2} + k_\gamma\delta\gamma = R_e + \int(fy - p\frac{\partial h}{\partial y}z_p)dA + S_y z_p. \tag{4}$$

where

$$S = \int (-\frac{h}{2}\nabla p + \mu V \frac{p}{(ph + 2\lambda p_a)}) dA \tag{5}$$

and

$$f = (p - p_a) + S_x \frac{\partial h}{\partial x} + S_y \frac{\partial h}{\partial y}. \tag{6}$$

The relation between h and the rotational angles is given by

$$h(x, y) = h_0 - \theta x + \gamma y + h_{rough}(x, y),$$

where $h_0 = h(0, 0)$.

The mean free path according to the Chapman-Enskog expansion is

$$\lambda = \frac{16}{5\sqrt{2\pi}} \frac{\mu}{p} \sqrt{R_{air} T}. \tag{7}$$

Under normal conditions this results in $\lambda_a = 0.065\mu$.

The arm attachment is chosen such that the slider rapidly responds to any possible asperities on the disk without damaging it. This results in very low spring constants in the simulation, thus high accuracy is needed in the computation due to cancellations. The only stiffness should be in the vertical motion so that the magnetic field generated by the recording head is well controlled. In this work we will only consider steady state solutions.

3. NUMERICAL IMPLEMENTATION

The equations were discretized using triangular elements of three, four and six nodes. The six node formulation uses isoparametric elements which allows for curvilinear boundaries and possible holes in the design.

In solving the Reynold's lubrication equation either p or the combination ph could be used as unknowns. The use of ph has a lower truncation error away from the rail sides and is more convenient for the time dependent computations. Though, the resulting CPU is slightly higher than using only p as unknown.

The actual discretization was obtained using Galerkin's approach. (A similar code which does not solve for the attitute although includes possible deformation of the slider was developed by Hendriks [6].) Each term in the Reynolds equation was discretized in the same manner. A similar discretization was used in the moment equations to yield a large non-linear system with unknowns p, θ, γ and h_0. The resulting Jacobian matrices were inverted using either a sparse matrix solver developed by Eisenstad et al. [7] and GMRES with an incomplete LU as preconditioner [8]. The sparse solver is slightly faster for matrices of up to 1000 unknowns, but for larger systems the iterative method is faster, see Fig. 2a. In order to save CPU time, the stiffness matrix was assembled only every four to five backsubstitutions.

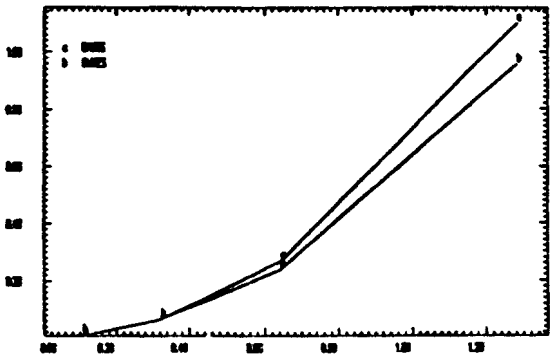

Fig. 2a: CPU Comparison of GMRES vs. Yale

The number of iterations in GMRES did depend on the number of vectors kept in the orthogonalization procedure. Fig. 2b shows the dependence of the number of iteration for varying number of orthogonalization vectors for 1095 unknowns.

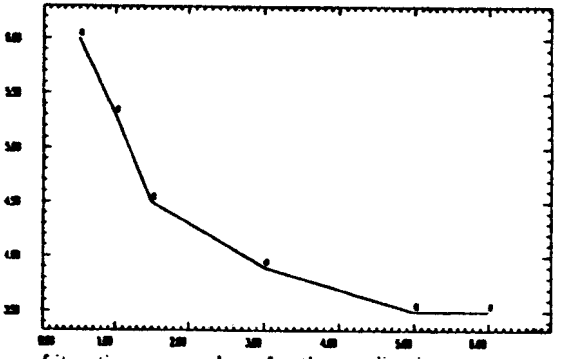

Fig. 2b: Number of iteration vs. number of orthogonalization vectors

The code has a simple minded mesh refinement. In order to determine which triangles need to be refined, a fictitious node is introduced in the center of each triangle and the Reynolds lubrication equation is solved at this new point, using as boundary data the values of the pressure at the corners of the triangle. When the difference between this value and the value of the interpolant at the center is greater than 1% the triangle is divided in either 3 or 4 triangles. Fig. 3a show the initial mesh. Fig. 3b shows the result of a mesh refinement procedure dividing each triangle in 3 new triangles, while Fig. 3c shows the result of using 4 new triangles. It becomes clear that the second approach leads to better meshes.

Fig. 3a: Initial Mesh

Fig. 3b: Mesh using subdivision by 3 triangles

Fig. 3c: Mesh using subdivision by 4 triangles

4. RESULTS

In this section we discuss the obtained results due to roughness and inertia effects.

4.1 INERTIA EFFECTS

The air-flow at the entrance of the taper can be regarded as two-dimensional on a scale of the taper height. The air is partially deflected upwards while a small amount is carried by the disk under the slider. At the stagnation point, air pressure rises by an amount corresponding to the dynamic pressure. A similar rise in pressure occurs for very small inlet gaps, i.e. very low local Reynolds number, and is usually termed ram effect (see Henshaw et al. [5]). This situation particularly arises in sliders at skew angle of attacks away from the front tapers.

We modify the pressure along the sides of the rails, to take into account the ram effect to read

$$p = p_a + \frac{1}{2}\rho_a U^2 + C\frac{\mu U}{h}, \tag{8}$$

where U is the normal component of the velocity at the boundary and h is the distance to the disk. The constant C is taken to be $C = 12.5$, to fit the data published in [5].

As the skew angle increases, the taper becomes less effective and the minimum flying height decreases, while the pitch angle increases. The ram effect becomes then even more important producing an increase in the minimum height and a decrease in the pitch angle of the solution without the inertia effects. Fig. 4a shows the pitch values and Fig. 4b show the roll values for Dirichlet pressure data and for the pressure values including ram effects.

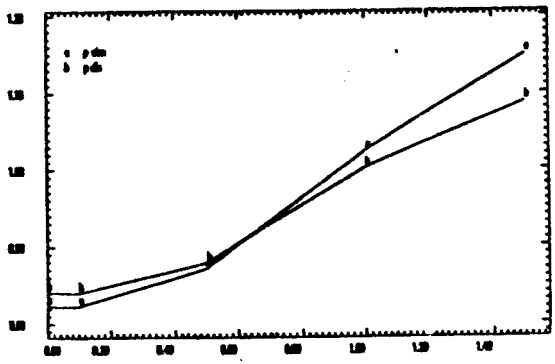

Fig. 4a: Pitch angle for varying skew angle

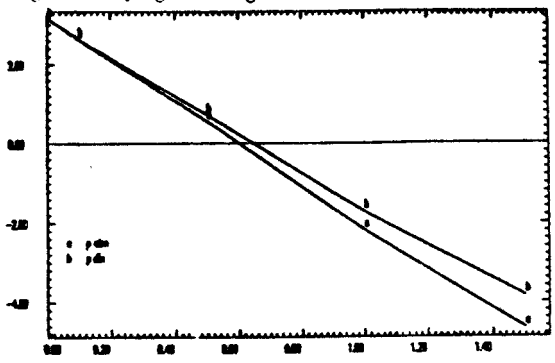

Fig. 4b: Roll angle for varying skew angle

4.2 ROUGHNESS EFFECTS

In this section we present some results of roughness on flying height. There are two different cases in the case of roughness and they arise from the relatives values of the bearing number

$$\Lambda = \frac{6\mu U L}{p_a h_{min}^2} \tag{9}$$

and the size of the roughness. Typical numbers for the bearing number are around 2000 while hard disks can be polished so that the peek to valley values of the roughness is around 0.025μ. The actual homogeneized equations can be found in the work by Greengard [9]. Our simulations fall into the case in which β is much smaller than Λ, where

$$h(x, y) = h(0, 0) - \theta x + \gamma y + \alpha \sin 2\beta\pi x. \tag{10}$$

In this case the homogenized pressure, in the one dimensional case, results in,

$$\frac{\partial}{\partial x}\left\{\bar{p}\left(\frac{1}{\bar{h}}\right)^{-1}\right\} = 0. \tag{11}$$

Fig. 5a shows the influence of longitudinal roughness for varying roughness size: here *alpha* = 0, 0.04, 0.08, 0.12 and 0.16μ, while β was kept at $12/L$.

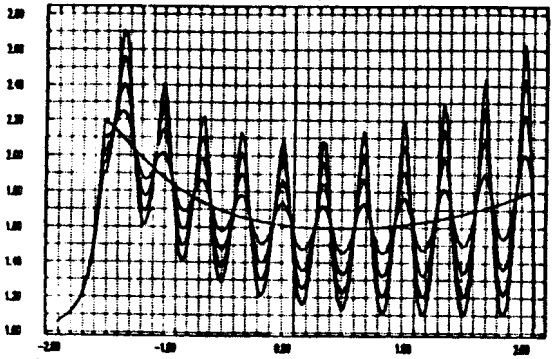

Fig. 5a: Pressure along center of rail for longitudinal roughness

Finally, Fig. 5b shows the minimum flying height vs. the β, the wave number of the roughness. We show results for $L\beta = 0, 4, 12, 24, 48, 96$ and 192. The largest computation involves 50128 nodes and 92496 elements.

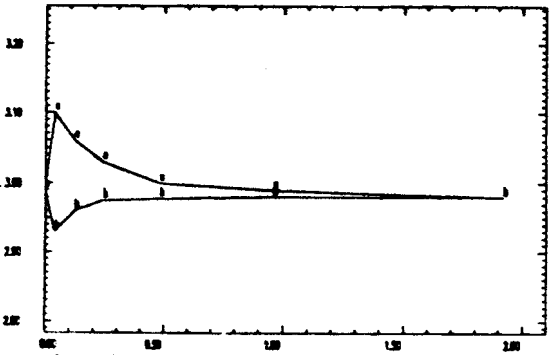

Fig. 5b: Minimum flying height vs. β for longitudinal roughness, for two different roughness phase

ACKNOWLEDGEMENTS

We thank IBM Argentina for providing the support for this work. We also would like to thank Dr. Andrés Saul, Lic. Jorge Sobehart and Pablo Dmitruk for interesting discussions. Dr. Ken Dechert was kind enough to provide with experimental and numerical data which was used to validate the current results.

NOMENCLATURE

h: distance between the bottom of the slider to the rotating disk
h_{eq}: height at equilibrium
h_{rough}: roughness
I_γ: slider moment of inertia for roll angle
I_ϕ: slider moment of inertia for pitch angle